JACS
JOURNAL OF THE AMERICAN CHEMICAL SOCIETY
Communication
pubs.acs.org/JACS

Chemical Mechanism of the Phosphotriesterase from *Sphingobium* sp. Strain TCM1, an Enzyme Capable of Hydrolyzing Organophosphate Flame Retardants

Andrew N. Bigley,[†] Dao Feng Xiang,[†] Zhongjie Ren,[‡] Haoran Xue,[†,§] Kenneth G. Hull,[†,§] Daniel Romo,[†,§] and Frank M. Raushel*[,†,‡]

[†]Department of Chemistry, Texas A&M University, College Station, Texas 77843, United States
[‡]Department of Biochemistry & Biophysics, Texas A&M University, College Station, Texas 77843, United States

Supporting Information

ABSTRACT: The mechanism of action of the manganese-dependent phosphotriesterase from *Sphingobium* sp. strain TCM1 that is capable of hydrolyzing organophosphate flame retardants was determined. The enzyme was shown to hydrolyze the R_P-enantiomer of *O*-methyl *O*-cyclohexyl *p*-nitrophenyl thiophosphate with net inversion of configuration and without the formation of a covalent reaction intermediate. These results demonstrate that the enzyme catalyzes the hydrolysis of substrates by activation of a nucleophilic water molecule for direct attack at the phosphorus center.

The recently discovered phosphotriesterase (PTE) from *Sphingobium* sp. strain TCM1 (*Sb*-PTE) is catalytically active against a broad range of substrates including organophosphate plasticizers and flame retardants.[1,2] The more commonly known neurotoxic organophosphate insecticides and nerve agents utilize a labile bond to facilitate their neurotoxic effects.[3] The flame retardants and plasticizers, such as triethylchlorophosphate (TECP) and tricresylphosphate (TCP), are extremely stable compounds that persist for long periods of time.[4,5] The use of these compounds as additives in plastics, foams and lubricants has led to significant concerns about toxicity and widespread dispersal in the environment. The well-known PTE from *Pseudomonas diminuta* (*Pd*-PTE) lacks measurable catalytic activity against the organophosphorus flame retardants and plasticizers.[2]

Sb-PTE is able to efficiently hydrolyze organophosphate triesters that *Pd*-PTE cannot hydrolyze.[1,2] The relative rates of hydrolysis of organophosphorus substrates by *Pd*-PTE exhibit a strong dependence on the pK_a of the leaving group, but the substrate profile for *Sb*-PTE does not.[6] For example, with *Pd*-PTE the k_{cat}/K_m for the hydrolysis of substrates with a phenolate leaving group is ~6-orders of magnitude lower than for a substrate with a *p*-nitrophenolate leaving group. The difference in reaction rates with *Sb*-PTE is less than 2-fold, and the best substrate currently known for *Sb*-PTE is triphenylphosphate.[2]

Pd-PTE utilizes a binuclear metal center to activate a bridging hydroxide for direct nucleophilic attack on the phosphorus center of the substrate.[7−9] However, the active site of *Pd*-PTE does not appear to provide a mechanism for protonation of the leaving group.[10] *Sb*-PTE has been shown to bind manganese in the active site and the lack of a strong dependence on the pK_a of the leaving group suggests that the mechanism for the delivery and removal of protons in the active sites of these two enzymes is different.[2]

While relatively little is currently known about the protein structure of *Sb*-PTE, homology modeling suggests that the protein folds as a 7-bladed β-propeller.[2] Two other known phosphotrieserases, human paraoxonase 1 (PON1) and squid diisopropyl fluorophosphatase (DFPase), are also known to have a β-propeller fold, and structural alignments among *Sb*-PTE, PON1 and DFPase suggest that the active sites of these enzymes are similar.[11,12] DFPase has been shown to utilize covalent catalysis, with an active site aspartate serving as the initial nucleophile resulting in a covalently bound intermediate, which is subsequently hydrolyzed by an attack of water on the carboxylate carbon of the aspartate side chain rather than the phosphorus center.[12] However, the overall stereochemical outcome at phosphorus for the hydrolysis of phosphate esters by either PON1 or DFPase has not apparently been experimentally determined. Since *Sb*-PTE can hydrolyze a broad range of toxic compounds that are not accessible as substrates by *Pd*-PTE, PON1, or DFPase, it is important to more clearly understand the molecular differences and similarities in the chemical mechanisms for substrate hydrolysis employed by these enzymes. Here we probe the mechanism of hydrolysis of phosphate esters by *Sb*-PTE by determination of the stereochemical course at phosphorus using a chiral thiophosphate substrate and by measurement of ^{18}O-incorporation into the product from solvent under single and multiple turnover conditions.

There are a variety of reaction mechanisms that are possible for the enzyme-catalyzed hydrolysis of organophosphate triesters. The most straightforward mechanism utilizes the direct nucleophilic attack of an activated water/hydroxide on the phosphorus center (Scheme 1a). For substrates with highly activated leaving groups, such as *p*-nitrophenol, it is also possible for the initial nucleophilic attack to occur on the aromatic ring of the leaving group with subsequent C−O bond cleavage through a nucleophilic aromatic substitution mechanism (not shown in detail), rather than breakage of the P−O

Received: December 6, 2015
Published: February 23, 2016

DOI: 10.1021/jacs.5b12739
J. Am. Chem. Soc. 2016, 138, 2921−2924

Scheme 1. Potential Chemical Mechanisms for *Sb*-PTE

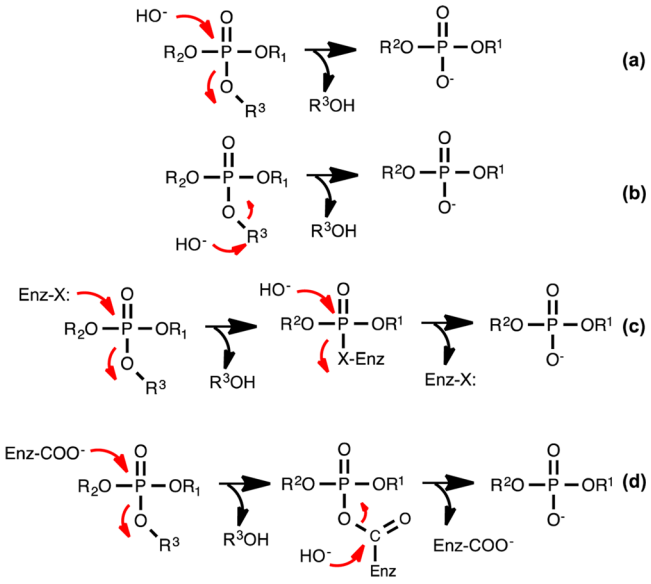

bond (Scheme 1b). Alternatively, the reaction may be initiated by an enzyme-based nucleophile that results in the formation of a covalent intermediate that is subsequently hydrolyzed by an activated water/hydroxide (Scheme 1c). If the enzyme-based nucleophile is the side chain carboxylate from either glutamate or aspartate, then hydrolysis of the covalent intermediate can occur either by nucleophilic attack at phosphorus or attack on the carboxylate carbon proceeding through a typical tetrahedral intermediate (Scheme 1d). These mechanisms can be distinguished from one another by determination of the stereochemical outcome at phosphorus and measurement of the isotopic composition of the products when the reaction is conducted in ^{18}O-labeled water.

To determine whether the initial nucleophilic attack is directed at the leaving group with C–O bond cleavage (Scheme 1b), *Sb*-PTE was used to catalyze the hydrolysis of paraoxon (diethyl *p*-nitrophenyl phosphate) in ^{18}O-labeled water under conditions of multiple turnovers. If C1 of the *p*-nitrophenyl group is attacked by water/hydroxide then the isolated *p*-nitrophenolate will have a nominal molecular mass of 140, rather than 138. Alternatively, if nucleophilic attack occurs at the phosphorus center, then the diethyl phosphate product will have a nominal mass of 155, rather than 153. As expected, when the hydrolysis reaction was conducted in unlabeled water the *p*-nitrophenolate was isolated with an m/z of 138 and diethyl phosphate at an m/z of 153 (Figure 1a). However, when the hydrolysis reaction was conducted under multiple turnover conditions in ~60% ^{18}O-labeled water, the *p*-nitrophenolate was produced with an m/z of 138, whereas the diethyl phosphate was isolated as a mixture of species with m/z values of 153 and 155 (Figure 1b). These results eliminate the mechanism depicted in Scheme 1b. Therefore, the reaction catalyzed by *Sb*-PTE occurs via the direct attack of a nucleophile at the phosphorus center of the substrate.

The attack at the phosphorus center can occur with an enzyme-activated water molecule or an enzyme-based nucleophile. If there is a direct attack by water, then the net stereochemical outcome at phosphorus is *inversion* of configuration (Scheme 1a). If the initial attack at phosphorus is via a nucleophile such as serine then the stereochemical

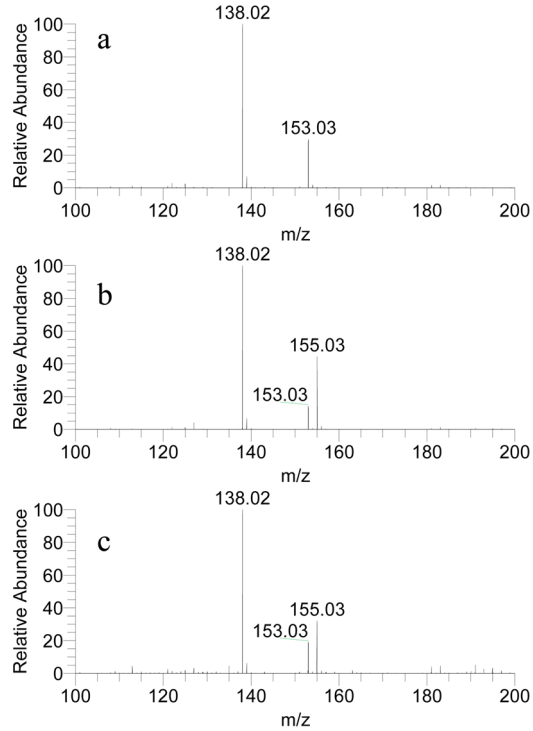

Figure 1. Mass spectra of *p*-nitrophenol and diethlyphosphate from the *Sb*-PTE catalyzed hydrolysis of paraoxon. (a) Control reaction conducted in unlabeled water. (b) Multiple turnover conditions where 500 μM paraoxon was hydrolyzed with 50 μM *Sb*-PTE in ~60% ^{18}O-labeled water. (c) Single turnover conditions in ~60% ^{18}O-labeled water where 50 μM paraoxon was hydrolyzed with 150 μM *Sb*-PTE. The peaks identified are unlabeled *p*-nitrophenolate (m/z = 138.02), unlabeled diethylphosphate (m/z = 153.03), and ^{18}O-labeled diethylphosphate (m/z = 155.03).

outcome is predicted to be *retention* of configuration (Scheme 1c). However, if the initial nucleophilic attack is via the carboxylate side chain of aspartate or glutamate, the net stereochemical outcome is either retention or inversion, depending on whether the mixed anhydride intermediate is ultimately attacked at phosphorus (Scheme 1c) or carbon (Scheme 1d).

The mechanism depicted in Scheme 1d can be interrogated in two ways. If the reaction is conducted in ^{18}O-labeled water under single turnover conditions, then the recovered diethyl phosphate will not contain an ^{18}O-label. When we utilized a 3-fold molar excess of *Sb*-PTE to hydrolyze paraoxon in ~60% ^{18}O-labeled water, the isotopic content of the recovered diethyl phosphate was essentially the same as the solvent (Figure 1c). The utilization of a side chain nucleophile from either glutamate or aspartate was also probed by measurement of ^{18}O-incorporation into the protein when hydrolysis of paraoxon was conducted in >95% ^{18}O-labeled water. After the substrate had been consumed, the enzyme was proteolyzed with trypsin and the resulting peptides analyzed by mass spectrometry. The net peptide coverage was 87% and no peptide was identified that had an M+2 or M+4 peak that differed significantly from that of the unlabeled control experiment (Table S1). The only peptides containing either glutamate or aspartate that were not identified by mass spectrometry were ^{181}DPR^{183}, ^{373}SQPKMRLVGEAK^{384}, and ^{499}IVDLR^{503}. These results are inconsistent with the mechanism depicted in Scheme 1d.

DOI: 10.1021/jacs.5b12739
J. Am. Chem. Soc. 2016, 138, 2921–2924

The differentiation between the mechanisms depicted in parts a and c of Scheme 1 was accomplished by determination of the net stereochemical outcome at phosphorus using *O*-methyl *O*-cyclohexyl *O*-(*p*-nitrophenyl) thiophosphate (**1**) as the chiral substrate. Previously, we have shown that *Pd*-PTE catalyzes the hydrolysis of chiral substrates with inversion of configuration at phosphorus.[7] We have also shown that for the hydrolysis of chiral substrates such as compound **1** that wild-type *Pd*-PTE will preferentially hydrolyze the R_P-enantiomer relative to the S_P-enantiomer and that the stereochemical preference for mutants such as G60A will be significantly greater than 100:1 for the R_P-enantiomer, relative to the S_P-enantiomer.[13] Therefore, the hydrolysis of a racemic mixture of compound **1** by the G60A mutant of *Pd*-PTE will result in the formation of the S_P-enantiomer of *O*-methyl *O*-cyclohexyl thiophosphate (**2**) as depicted in Scheme 2.

Scheme 2. Hydrolysis of (R_P)-*O*-Methyl *O*-Cyclohexyl *O*-(*p*-Nitrophenyl) Thiophosphate (1) to (S_P)-*O*-Methyl *O*-Cyclohexyl Thiophosphate (2) by *Pd*-PTE

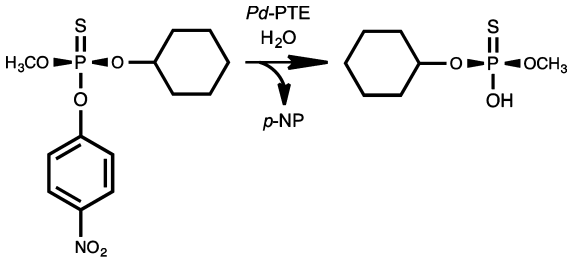

The stereoselective hydrolysis of racemic **1** by the G60A mutant of *Pd*-PTE is graphically illustrated in Figure 2. After the addition of 12 nM of this mutant to a 25 μM mixture of racemic compound **1**, only ~50% of the substrate is hydrolyzed after a period of ~1000 s (blue trace). Addition of the *Pd*-PTE mutant VRN-VQFL-I106G/L308S, a variant known to preferentially hydrolyze the opposite enantiomer than G60A, hydrolyzes the remaining S_P-enantiomer of compound **1**.[14] When hydrolysis of racemic **1** was initiated by the addition of 34 nM *Sb*-PTE, the reaction stopped after ~50% of the substrate was consumed (Figure 2, red trace). Addition of the G60A variant of *Pd*-PTE resulted in no further hydrolysis of the substrate. This result demonstrates that *Sb*-PTE and the G60A variant of *Pd*-PTE preferentially hydrolyzed the same enantiomer of compound **1**. When the VRN-VQFL-I106G/L308S variant of *Pd*-PTE was added to the reaction mixture, the remaining portion of the substrate was hydrolyzed, thus confirming that *Sb*-PTE and G60A *Pd*-PTE have strong stereochemical preferences for hydrolysis of the same enantiomer of compound **1**.

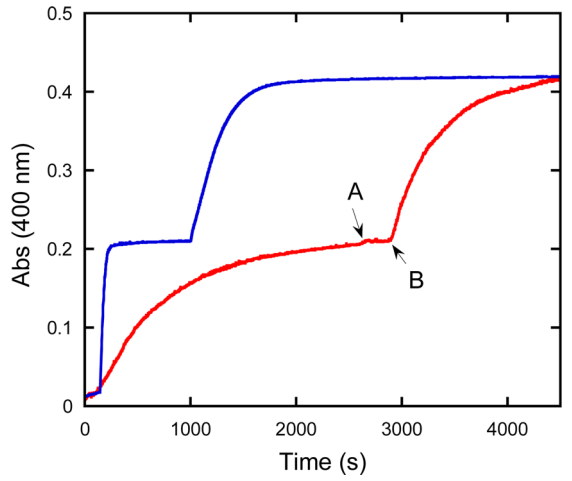

Figure 2. Stereoselective hydrolysis of 25 μM *O*-methyl, *O*-cyclohexyl *p*-nitrophenylthiophosphate (**1**) by *Pd*-PTE and *Sm*-PTE. The blue trace illustrates the time course for the hydrolysis of **1** by the G60A variant of *Pd*-PTE (12 nM), which selectively hydrolyzes the R_P-enantiomer, while the second phase is due to the addition of the VRN-GVQF mutant of *Pd*-PTE (770 nM), which hydrolyzes the S_P-enantiomer. The red trace shows the time course for the hydrolysis of the R_P-enantiomer by *Sb*-PTE (34 μM). At time point A (time =2600−2900 s) 12 nM of G60A *Pd*-PTE was added to the reaction mixture and there was no further hydrolysis. At time point B (time =2900 s) the VRN-GVQF mutant of *Pd*-PTE (770 nM) was added resulting in hydrolysis of the S_P-enantiomer.

The stereochemistry of the product produced by the hydrolysis of the R_P-enantiomer of compound **1** by *Sb*-PTE was determined by ^{31}P NMR spectroscopy using the chiral shift reagent (*S*)-α-methylbenzylamine.[15] When racemic compound **1** was completely hydrolyzed by a combination of the G60A and L7ep3aG variants of *Pd*-PTE, the racemic product, *O*-methyl *O*-cyclohexyl thiophosphate (**2**) gave separate ^{31}P NMR resonances for each of the two enantiomers because of the differential interactions with the chiral shift reagent. Resonances appeared at 56.54 and 56.49 ppm (Figure 3a). When hydrolysis of racemic **1** was initiated by the addition of the G60A variant of *Pd*-PTE, only a single resonance was observed at 56.54 ppm, due to the selective formation of the (S_P)-*O*-methyl *O*-cyclohexyl thiophosphate product (Figure 3b). The unreacted substrate from the hydrolysis of racemic **1** by the G60A mutant of *Pd*-PTE was isolated after ~45% of the original reaction mixture had been hydrolyzed. The substrate was subsequently hydrolyzed by the L7ep3aG mutant of *Pd*-PTE. The ^{31}P NMR spectrum of the reaction products shows a major resonance at 56.49 ppm, which is attributed to the formation of (R_P)-*O*-methyl *O*-cyclohexyl thiolphosphate (**2**) and a minor peak at 56.54 ppm for the (S_P)-enantiomer of compound **2** (Figure 3c).

When *Sb*-PTE was used to hydrolyze a racemic mixture of *O*-methyl *O*-cyclohexyl *O*-(*p*-nitrophenyl) thiophosphate (**1**), only a single resonance was observed at ~56.54 ppm, which corresponds to the formation of (S_P)-*O*-methyl *O*-cyclohexyl thiophosphate (Figure 3d). When this sample was mixed in a 1:1 ratio with the reaction product produced by the hydrolysis of racemic **1** catalyzed by the G60A variant of *Pd*-PTE, only a single resonance appeared, confirming that the product catalyzed by *Sb*-PTE and the G60A variant of *Pd*-PTE are the same (Figure 3e). The identity of the single reaction product was further confirmed by spiking the reaction mixture from the *Sb*-PTE- and G60A *Pd*-PTE-catalyzed reactions with the product produced by the reaction catalyzed by the L7ep3aG variant of *Pd*-PTE (Figure 3f).

Sb-PTE selectively hydrolyzes the R_P-enantiomer of compound **1** and catalyzes the formation of the S_P-enantiomer of the product **2**. This result demonstrates that the enzyme-catalyzed reaction proceeds with inversion of configuration at phosphorus. The reaction mechanism must therefore involve the activation of a solvent water molecule for the direct nucleophilic attack on the phosphorus center and a covalent reaction intermediate is not involved in substrate turnover.

In this Communication we have demonstrated that the reaction catalyzed by *Sb*-PTE proceeds with a direct attack of

DOI: 10.1021/jacs.5b12739
J. Am. Chem. Soc. 2016, 138, 2921−2924

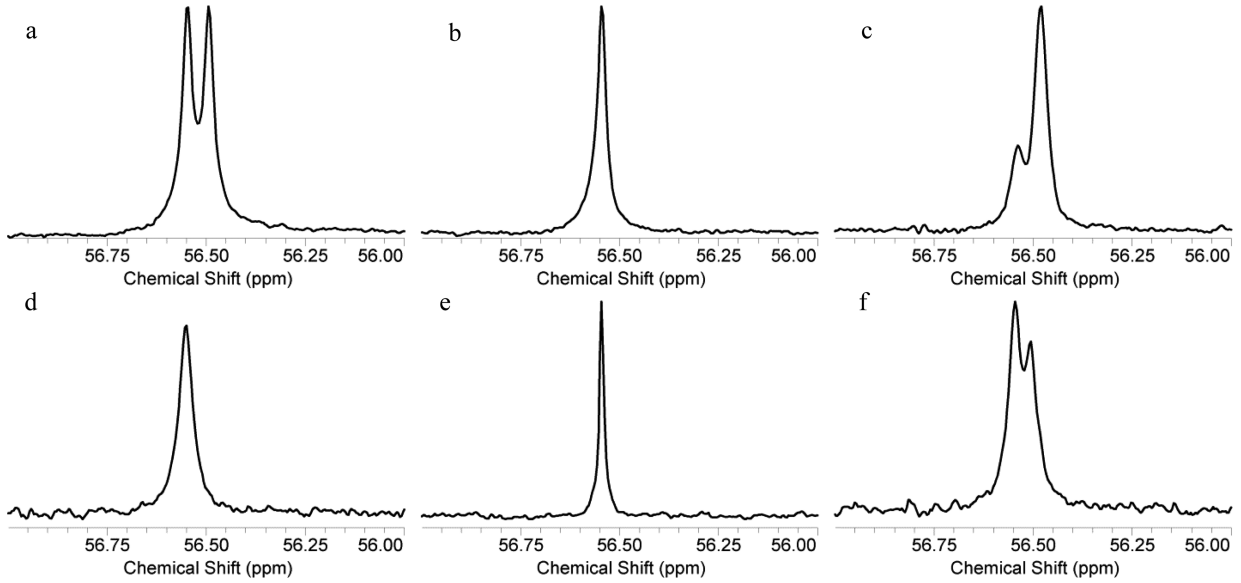

Figure 3. ^{31}P NMR spectra of the products of hydrolysis of racemic *O*-methyl *O*-cyclohexyl *p*-nitrophenylthiophosphate (**1**) in the presence of the chiral shift agent (*S*)-*α*-methylbenzylamine in $CDCl_3$. (a) Total hydrolysis of racemic **1** by *Pd*-PTE. (b) Hydrolysis product of racemic **1** catalyzed by the G60A variant of *Pd*-PTE (R_p-enantiomer of compound **2**). (c) Product from the hydrolysis of compound **1** as catalyzed by the L7ep3aG variant of *Pd*-PTE (S_p-enantiomer of compound **2**). (d) Product from the hydrolysis of racemic **1** catalyzed by *Sb*-PTE. (e) A mixture of the hydrolysis products produced by the hydrolysis of racemic **1** by the G60A mutant of *Pd*-PTE and of *Sb*-PTE. (f) A mixture of hydrolysis products of the G60A mutant of *Pd*-PTE, *Sb*-PTE, and the L7ep3aG-*Pd* mutant of PTE.

water on the phosphorus center that results in an inversion of stereochemistry at phosphorus (Scheme 1a). This phosphotriesterase is unusual in its ability to hydrolyze organophosphate triesters with unactivated leaving groups. This observation suggests that the catalytic mechanism for the protonation of the leaving group in the transition state must be significantly different from that observed with other PTEs, such as the well-characterized one from *Pseudomonas diminuta*. Efforts are currently underway to determine the three-dimensional crystal structure by X-ray diffraction methods.

■ ASSOCIATED CONTENT

Supporting Information

The Supporting Information is available free of charge on the ACS Publications website at DOI: 10.1021/jacs.5b12739.

Additional methods, and NMR and mass spectral data (PDF)

■ AUTHOR INFORMATION

Corresponding Author

*raushel@tamu.edu

Present Address

§H.X., K.G.H., and D.R.: Department of Chemistry and Biochemistry, Baylor University, Waco, TX 76798.

Notes

The authors declare no competing financial interest.

■ ACKNOWLEDGMENTS

This work was supported in part by the Defense Threat Reduction Agency (HDTRA1-14-1-0004) in a grant to F.M.R. The Natural Products LINCHPIN Laboratory at Texas A&M University was supported by the College of Science and the Office of the Vice President for Research.

■ REFERENCES

(1) Abe, K.; Yoshida, S.; Suzuki, Y.; Mori, J.; Doi, Y.; Takahashi, S.; Kera, Y. *Appl. Environ. Microbiol.* **2014**, *80*, 5866.
(2) Xiang, D. F.; Bigley, A. N.; Ren, Z.; Xue, H.; Hull, K. G.; Romo, D.; Raushel, F. M. *Biochemistry* **2015**, *54*, 7539.
(3) Maxwell, D. M.; Brecht, K. M.; Koplovitz, I.; Sweeney, R. E. *Arch. Toxicol.* **2006**, *80*, 756.
(4) Reemtsma, T.; Quintana, J. B.; Rodil, R.; Garcia-Lopez, M.; Rodriguez, I. *TrAC, Trends Anal. Chem.* **2008**, *27*, 727.
(5) van der Veen, I.; de Boer, J. *Chemosphere* **2012**, *88*, 1119.
(6) Hong, S. B.; Raushel, F. M. *Biochemistry* **1996**, *35*, 10904.
(7) Lewis, V. E.; Donarski, W. J.; Wild, J. R.; Raushel, F. M. *Biochemistry* **1988**, *27*, 1591.
(8) Samples, C. R.; Howard, T.; Raushel, F. M.; DeRose, V. J. *Biochemistry* **2005**, *44*, 11005.
(9) Vanhooke, J. L.; Benning, M. M.; Raushel, F. M.; Holden, H. M. *Biochemistry* **1996**, *35*, 6020.
(10) Aubert, S. D.; Li, Y.; Raushel, F. M. *Biochemistry* **2004**, *43*, 5707.
(11) Ben-David, M.; Elias, M.; Filippi, J. J.; Dunach, E.; Silman, I.; Sussman, J. L.; Tawfik, D. S. *J. Mol. Biol.* **2012**, *418*, 181.
(12) Blum, M. M.; Lohr, F.; Richardt, A.; Ruterjans, H.; Chen, J. C. *J. Am. Chem. Soc.* **2006**, *128*, 12750.
(13) Tsai, P. C.; Bigley, A.; Li, Y.; Ghanem, E.; Cadieux, C. L.; Kasten, S. A.; Reeves, T. E.; Cerasoli, D. M.; Raushel, F. M. *Biochemistry* **2010**, *49*, 7978.
(14) Bigley, A. N.; Mabanglo, M. F.; Harvey, S. P.; Raushel, F. M. *Biochemistry* **2015**, *54*, 5502.
(15) Mikolajczyk, M.; Omelanczuk, J.; Leitloff, M.; Drabowicz, J.; Ejchart, A.; Jurczak, J. *J. Am. Chem. Soc.* **1978**, *100*, 7003.

DOI: 10.1021/jacs.5b12739
J. Am. Chem. Soc. 2016, 138, 2921−2924